

Optimization of data centre waste heat integration into the low-temperature district heating networks

Josip Miškić^{1*}, Hrvoje Dorotić², Tomislav Pukšec¹, Vladimir Soldo¹, Neven Duić¹

¹*The University of Zagreb, Faculty of Mechanical Engineering and Naval Architecture,*

Department of Energy, Power Engineering and Environmental Engineering, Ulica Ivana Lučića 5, 10002, Zagreb, Croatia

²*Energy Institute Hrvoje Požar, Savska cesta 163, 10000, Zagreb, Croatia*

**email: josip.miskic@fsb.hr*

Abstract

The number of data centres (DC) in recent years is growing rapidly, and with that, the share in total consumption of electricity is growing too. A significant amount of electricity is transformed into heat energy which increases the optimal temperature in DC for component operation. This heat needs to be removed and usually, it doesn't have any further application. Today it is recognized that waste heat can be integrated into district heating (DH) and by using it reduce the usage of conventional heat fuels. Integration of waste heat is possible in three ways: with a heat exchanger (HEX), with a booster heat pump (BHP), or with the combination of the HEX and heat pump. In this paper, a combination of HP and HEX was used. Although those utilizations are examined and implemented, there is a lack of research on the optimization of the integration of waste heat into the district heating network (DHN). To perform optimization, a thermodynamic model of the DC and a pinch analysis model were developed. In this study, a method for evaluating the economic feasibility of DC waste heat integration into DH systems is proposed. The most suitable integration technology of waste heat into DH systems by using the hourly merit order of waste heat utilization technologies based on pinch analysis is found. The connection pipe between DC and DHN is optimized, and the ideal diameter is determined considering different temperature regimes of the network: low-temperature, ultralow temperature, and neutral temperature networks. The methodology was tested using a case study of a DC in the City of Zagreb.

Keywords: *district heating, waste heat, data centre, pinch analysis, optimization, techno-economic assessment*

1. Introduction

Climate change is receiving increasing attention at the global, European, and local levels. People's awareness of the necessity of action is growing, and action to achieve carbon neutrality and hold the trend of increasing average global temperature can't be delayed. Policies are aiming to encourage energy transition which sets the same or at least similar goals for all energy sectors, namely: increasing the share of renewable energy sources, decarbonization, improving energy efficiency, electrifying services, and assets, and promoting digitalization and transparency of services. Under the influence of these goals is the District Heating & Cooling (DHC) sector [1], [2]. DHC has great potential for achieving the above-mentioned goals and one of the ways to accomplish them is to use waste heat. A DHN is in a densely populated urban area where are various urban heat sources, such as cooling systems in supermarkets, shopping malls, subways, DC, etc. These urban heat sources are significant sources of waste heat, and it is estimated that 1.2 EJ (1 EJ = 10^{18} J) of waste heat is available for integration into DH systems [3].

With the increasing digitalization of services, DC is becoming important worldwide and it is expected that the role of DC will be crucial in the future. Raise in the number of the DC, due to the rising demand for data storage, has necessary effects on energy consumption, i.e., consumption of electric energy. It is estimated that the consumption of DC takes a part of 1 % of total electric energy consumption worldwide and it will grow [4]. Many studies were carried out on the topic of waste heat recovery DC, especially on how to organize HVAC (Heating, Ventilating, and Air Conditioning) systems to achieve the highest possible integration of waste heat in DHN.

2. Literature review

The study from Fu and al. [5] presented a low-carbon DH system that features a low return water temperature, and the use of low-grade waste heat as the main heat source. This low-carbon DH system is developed for large cities, large waste heat sources, high heating densities, and the utilization of using large heating networks. The study shows that clean heating systems have great potential to reduce energy use, reduce emissions and improve the DH system economics. Ebrahimi et. al. in [6] provided a comprehensive review of all available waste heat reuse techniques used in DC. They detected two main electric energy consumers in DC: Information Technologies (IT) systems, used for processing and storage of data, and HVAC systems. The HVAC system needs to ensure a working environment in a set range for the proper functioning of IT equipment. The study offers a comparison between the technologies, and operational requirements and identifies the most suitable solution for waste heat reuse. The study from Rasmussen et al. [7] quantified and specified heat load and cooling infrastructure in and for DC. Heat dissipated in DC may vary depending on the performance of the devices. The study differs two types of DC: conventional DC – heat dissipation rates in the range of 430 – 861 W/m², and high-tech DC – heat dissipation rates in the range of 6.458 – 10.764 W/m². Huang et al, [8] in their research recognized variations in DC heat dissipation rates and proposed three main cooling techniques in DC: Air-cooled systems – used in small conventional DC, low-quality waste heat; water-cooled systems – used in mid and large-scale DC, high-quality waste heat; two-phase cooled systems – used in large-scale DC, high-quality waste heat. A wide range of dissipated heat presents a significant amount of waste heat that can be captured and reused. They find out that 68 % of dissipated heat can be recovered. Heat dissipation increases powering and cooling cost of DC, while the reuse of the waste heat energy can potentially reduce operational costs. To integrate waste heat from DC, Oro et al. in [9], studied two most common ways: integration from the return hot aisle or the chiller condenser. Waste heat recovery in the return hot aisle is usually implemented in CRAH (Computer Room Air Handler) cooling systems since the hot air streams in IT facility rooms are gathered at relatively high temperatures (about 45 °C) and delivered in a common duct to the air-handling units. The return hot air will be cooled down in an air-to-water HEX, this reduces cooling needs from the chiller in the CRAH system. Warm water from HEX feeds the evaporator in HP in which the temperature level of waste heat is increased. This study resulted in the evaluation of the potential heat reuse in air-cooled DC using different technologies and the development of dynamic energy models. In [10] Lennermo et al. studied feed-in systems. They proposed different ways of connecting the waste heat sources and the DH systems. They considered four main ways of the connection: Return/Supply: the water is withdrawn from the return pipe, heated to a correct temperature, and fed back into the supply pipe; Return/Return: the water is withdrawn from the return pipe, heated to any temperature higher than the temperature on the return line, and fed back into the return pipe; Supply/Return: the water is withdrawn from the supply pipe, heated to any temperature, it has already a higher temperature than the temperature in the return line, and fed back into the return pipe; Supply/Supply: the water is withdrawn from the supply pipe, heated to any temperature higher than the temperature on the supply line, and fed back into the supply pipe. The main contribution of this study is

an understanding of the challenges of feed-in systems. In [11] authors gave the hourly distribution of operating modes of cooling systems in DH. They found out that cooling systems will mostly operate during summer, while for the rest of the year outdoor air will be used for cooling. Davies et al. [12] made research on the topic of improving energy efficiency in DC, i.e., cooling and waste heat reuse systems. The focus was on boosting waste heat using HP and evaluation of this principle through energy and carbon emissions saving. A case study considered the new DHN that has been proposed for London. They found that large-scale reductions in energy use and carbon emissions are possible when DC is integrated into DHN. They discovered that integration of 3.5 MW DC in DHN can lead to savings of over 4.000 tonnes of CO₂ and nearly 1.5 mil. € annually. Wahlroos et al. [13] studied the utilization of DC waste heat in DHN and the impact on as well as the prospect for low-temperature DHN. The study finds out that DC is a reliable source of heat that is available during each hour of the day. Integration of DC in DHN could save from 0.6 % to 7.3 % total operational cost of DH prosumers which is economically feasible.

Through the literature review, it has been found that DC waste heat has significant potential for integration into DHN and there are a few main advantages:

- DCs are usually located in urban areas close to energy prosumers and consumers.
- Heat load is almost constant throughout the years, i.e., there is always an available amount of waste heat.
- The temperature level of waste heat is 30°C to 50°C.
- Technology for heat recovery and integration into DHN is mature.
- The operational cost of DC may be reduced.
- Energy and CO₂ savings on the side of the DH operator could be achieved [14], [15].

Based on the literature review, it is established that there are characteristics of DC waste heat integration that have not been investigated at all or are neglected. First, it is noticed that there are no valid thermodynamic models of DC that consider the potential of waste heat and the temperature level on an hourly basis. It is recognized that researchers usually don't consider the scenario analysis of the waste heat integration into DH systems, i.e., the different temperature regimes of low-temperature DH systems have not been considered. Also, we have noticed that many papers consider BHP and HEX as separate systems, i.e., the coupling of BHP and HEX in the waste heat integration system has not been considered yet. Therefore, the contribution of this research is:

- The thermodynamic model that calculates the amount and temperature level of waste heat on an hourly basis,
- The pinch model adapted to the DC thermodynamic model to maximize the amount of waste heat integration considering the pinch temperature difference, and temperature regimes of a DH system,
- Optimization of the ideal diameter of the connecting pipe by considering different low-temperature regimes,
- Cost calculation depending on the distance between the DC waste heat source and DHN,
- Cost comparison of waste heat integration concerning different temperature regimes in the DH system and integration technologies,
- DHN expansion potential calculation based on the amount of integrated waste heat from the DC.

This research aims to contribute to better energy planning of waste heat integration in DH systems by using pinch analysis. As a case study, the City of Zagreb was chosen. In Section 2 the Method and Input data are given, then in Section 4 the Results with accompanying discussion are presented. Finally, in Section 5 a Conclusion with a proposal for future research is given.

3. Method

The method is divided into three main steps as shown in Figure 1. First, to calculate the available waste heat from the DC as well as to calculate the temperature level of that waste heat, a waste heat model was created based on input data collected from literature and databases. Available heat and heat temperature serve as input data for pinch analysis. In the second step, pinch analysis calculates the hourly level of the integrated waste heat using HEX and BHP. A simpler version of this approach can be found in [16]. The observed waste heat integration system is located between the water-cooled chiller condenser and the cooling tower. Finally, the economic analysis was carried out, and the results were presented.

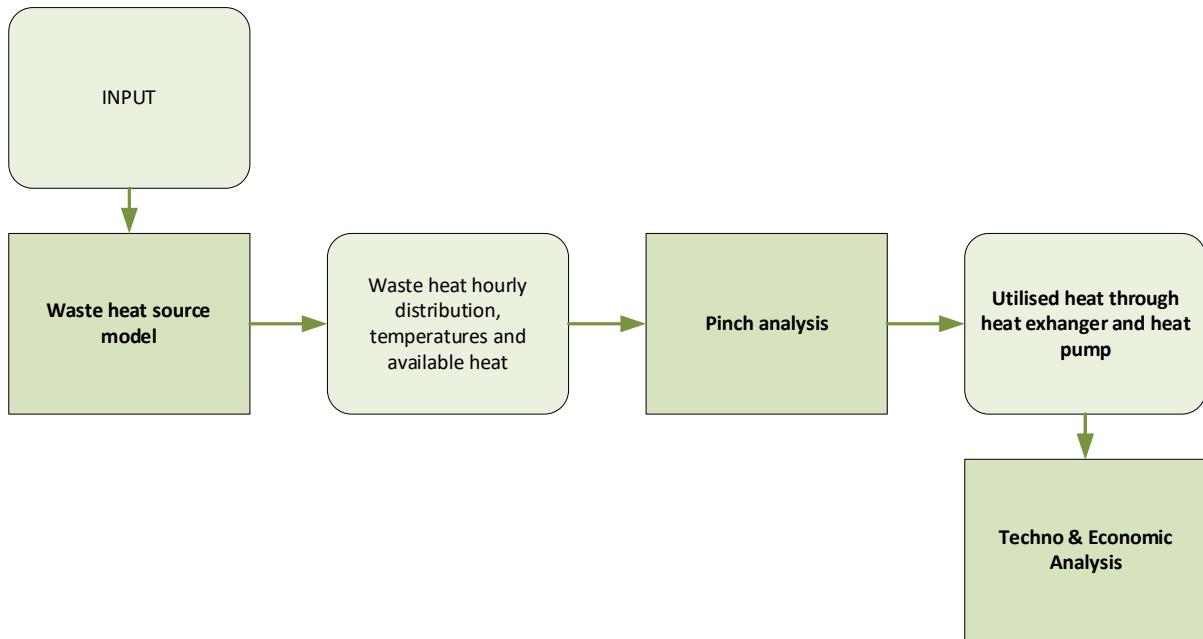


Figure 1 Method overview

The time variable approach is presented in the next subsection.

3.1. Time variable method

The time variable is considered as shown in Figure 2. The analysis and calculation were conducted for over one year with a time step of one hour. The first-time variable is calculated using the associated input data, such as load and ambient temperature. Utilized heat, $Q(t)_{utilised}$, is calculated by the model utilizing input data, pinch analysis, and considerations for the temperature of the waste heat source and the amount of available waste heat. Utilized heat is the total of heat used with HP, $Q(t)_{HP_{utilised}}$, and heat used with HEX, $Q(t)_{HEX_{utilised}}$. By adding a time step to the preceding time variable, the subsequent time variable needed to calculate the amount of heat used is obtained. The calculation is carried out once more with a new time variable. The calculation is repeated until the time variable reaches a value of 8760 hours. The total amount of heat used over a year is computed by adding up all the calculated amounts. For additional calculations, such as sensitivity and techno-economic analysis, the amount of used heat is required.

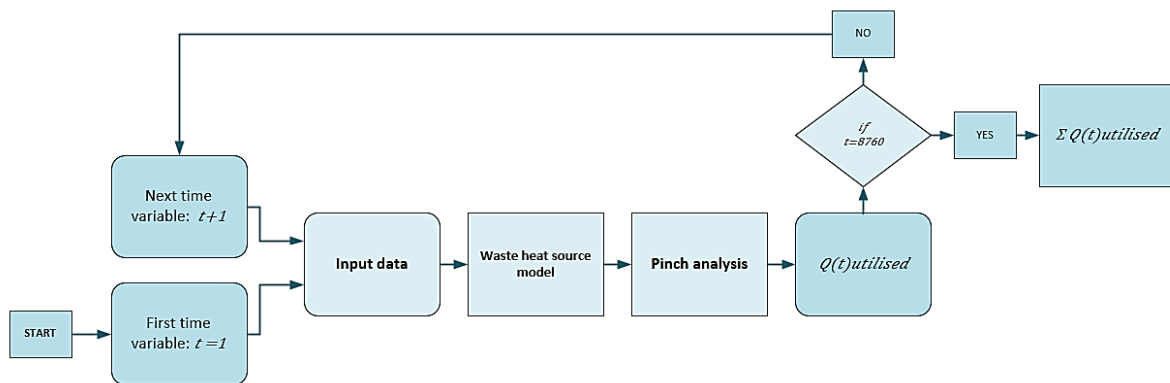


Figure 2 Time variable method overview

This time-variable approach makes it possible to know the conditions of HEX and BHP at any time of the year, including load, ambient temperature, waste heat source temperature, and available heat.

3.2. Data centre cooling

The DC is characterized by high heat dissipation rates due to the high capacity of operating IT devices and it is necessary to take away this heat using a cooling system. Since DC differ in their capacity different cooling technologies have been developed. There are three most common cooling technologies:

- Air-cooled systems,
- Water-cooled systems,
- Two-phased cooled systems.

In this research, the focus is on the most used ones in DC, air-cooled systems. The cold air aisle enters the server, heats up, and the hot air aisle exits. There are four configurations of air-cooled DC: computer room air conditioner units (CRAC) used in medium and large DC (capacity between 1000 and 2000 kW), Computer room air handler units (CRAH) used in large DC (capacity higher than 2000 kW), in-row cooling and rear door cooling used in small DC (capacity less than 1000 kW) [9].

The subject of research in this paper is the CRAH systems as shown in Figure 3.

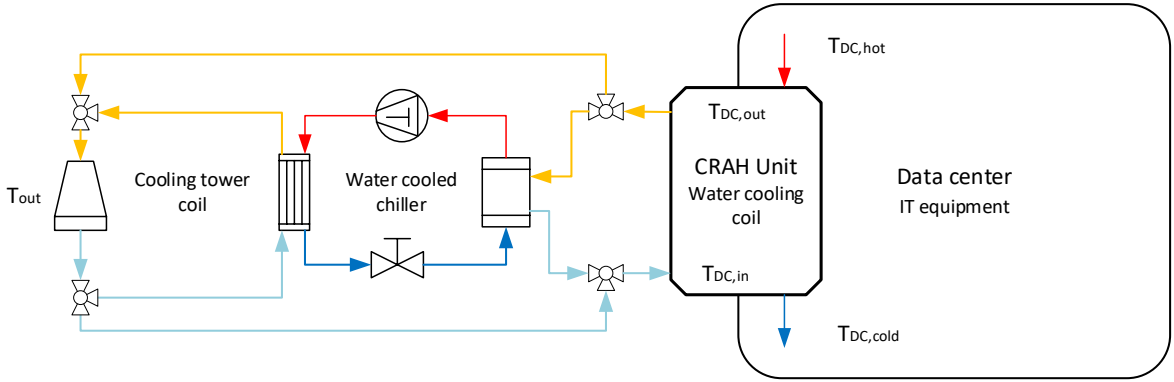


Figure 3 Data centre CRAH cooling system

The main components of the cooling system are the CRAH unit, water-cooled chiller, and cooling tower. An aisle of cooled air, $T_{DC,cold}$, enters the racks and absorbs heat to meet the set internal DC conditions. A heated air aisle, $T_{DC,hot}$, enters the CRAH unit where heat is transferred to the water circuit respecting the minimum required temperature difference for heat exchange. The heated water can then be cooled in two cooling modes depending on the outdoor wet-bulb temperature conditions, T_{wb} . In this paper to simplify the terminology the term outdoor temperature, T_{out} , is further used for T_{wb} . The two cooling modes we can distinguish are Free Air Cooling (FAC) and Forced Cooling (FC). Furthermore, to be able to determine which mode is operational it is necessary to know the inlet temperature of the cooling water, $T_{DC,in}$ in the CRAH unit and the pinch point temperature difference of the HEX in the CRAH unit [17].

FAC mode is a mode in which the cooling water is cooled on the cooling tower, i.e., outdoor air is used to cool the cooling water bypassing the water-cooled chiller. This cooling mode is used when the outdoor temperature is lower than the inlet DC temperature. The cooling capacity in this mode is determined by the capacity of the HEX in the cooling tower. The HEX in the cooling tower is designed to respect the pinch temperature difference, $\Delta T_{PPTD,rated}$, which is the minimum required temperature difference between the outdoor temperature and the cooling water temperature at the inlet to the CRAH unit. Therefore, the following condition for FAC cooling modes is set [17]:

$$T_{out} < T_{DC,in} - \Delta T_{PPTD,rated} \quad (1)$$

FC mode is a mode used for conditions when the outdoor temperature cannot meet the DC cooling needs. This mode occurs at high outdoor temperatures (well above inlet DC temperature), and the water-cooled chiller operates at full load. The set condition for the appearance of FC mode is [17]:

$$T_{out} \geq T_{DC,in} - \Delta T_{PPTD,rated} \quad (2)$$

Different DC cooling modes result in waste heat variation throughout the year and at different temperature levels. This is important for waste heat integration in DHN, and it is discussed in detail in the next subsection.

3.3. Waste heat recovery for district heating

The amount and temperature level of waste heat from DC depends on the cooling mode so the question arises which is the optimal way to integrate waste heat into DHN. The subject of this research is waste heat integration from CRAH systems. It is recognized that this type of cooling offers two ways to utilize and integrate waste heat into DHN. The first way to use it is to install the waste heat recovery system in the return hot air aisle at the exit of the server. The second way to integrate waste heat is to have the recovery system installed after the water-cooled chiller condenser [8], [9].

The waste heat recovery system from the chiller condenser is the subject of this paper and it is shown in Figure 4. This waste heat recovery system requires the installation of an additional coolant/water HEX in a cooling system. Also, this system is characterized by larger amounts of waste heat and higher temperature levels of the waste heat [8].

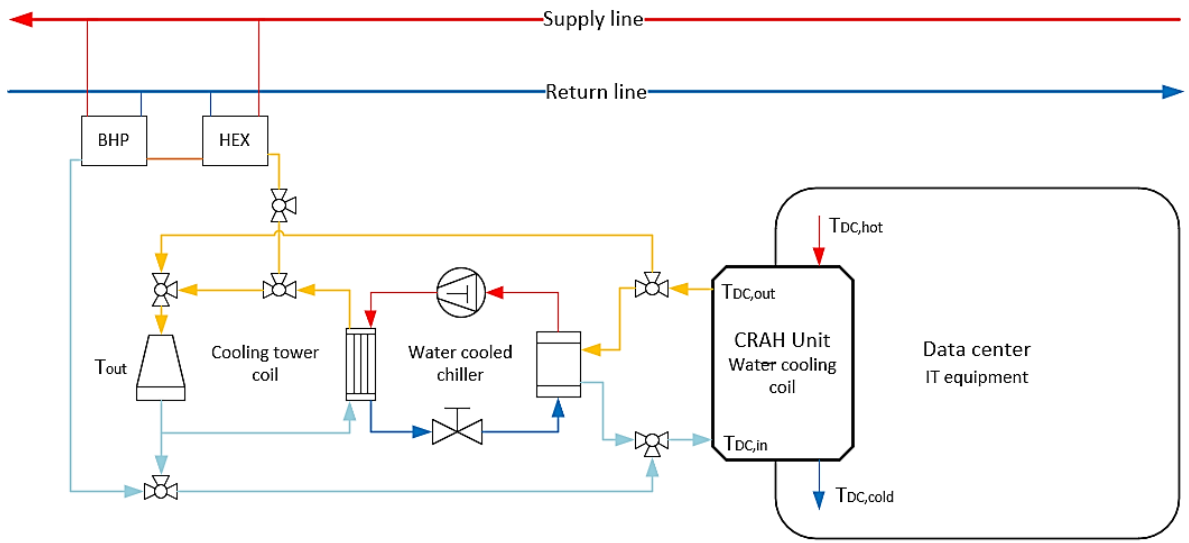


Figure 4 Waste heat integration from the chiller condenser side

3.4. Data centre Thermodynamic model

The model of waste heat from DC is made based on the literature review from which the input data is determined. The developed model offers two approaches for annual waste heat distribution calculation:

- I. Approach - Approach based on knowing the Specific DC power density, W_{DC} , and DC surfaces, A_{DC} . This data serves as input data for further calculation flow.
- II. Approach - Approach based on knowing the capacity of IT equipment, W_{IT} , and the capacity of other electrical systems in DC, W_{es} .

Depending on the chosen approach with which we enter the thermodynamic model, the total DC power capacity, P_{DC} , is calculated in the following way.

If Approach I is chosen, the power capacity is calculated as follows:

$$P_{DC} = W_{DC} * A_{DC}, [kW] \quad (3)$$

If Approach II is used, then power capacity is calculated as follows:

$$P_{DC} = W_{IT} + W_{es}, [kW] \quad (4)$$

Based on the literature and empirical data, it has been established that DC has an almost constant load during the year with a very small amplitude of variations [18].

Since the power loss in DC servers is 2 to 3%, they are negligible, and therefore the power load is equal to the cooling load. Cooling load is a source of waste heat, i.e., it is the heat that needs to be removed from DC to maintain the internal temperature in an acceptable range [8]. Therefore Equation 6 is valid and shows that in each hour the cooling load is equal to the DC load:

$$\phi_{CL} = P_{DC}, [kW] \quad (5)$$

Where ϕ_{CL} is cooling load. Based on Equation 5, the annual accumulated cooling load, Φ_{CL} , is calculated as follows:

$$\Phi_{CL} = \sum_{i=1}^{8760} \phi_{CL}, [kWh] \quad (6)$$

In the next step, based on the ambient temperature and conditions set in Equations 1 and 3, the cooling mode is determined. This allows the calculation of the total operating hours of each cooling mode. t_{FAC} represents the total operating hours of the FAC mode, while t_{FC} presents the total operating hours of the FC mode. The operating hours of cooling modes are dependent on local climatic conditions. Figure 5 shows an example of the distribution of cooling modes as a function of time [17].

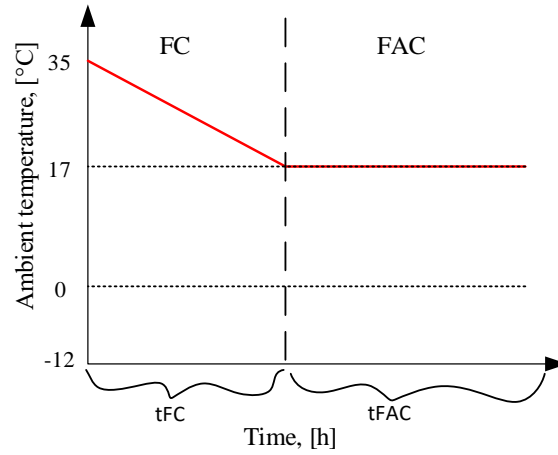


Figure 5 Cooling modes distribution

In the next step, the waste heat released throughout each cooling mode is calculated. In the FAC mode, the hourly amount of waste heat is equal to the cooling load, and the total annual amount of waste heat available through FAC mode, $Q_{WH,FAC}$, is obtained by summing the hourly amounts of waste heat as shown in Equation 7.

$$Q_{WH,FAC} = \sum_{i=1}^{8760} \phi_{CL}, [kWh] \quad (7)$$

In FC mode, the heat from DC is first going through a water-cooled chiller and then released through the cooling tower. The released heat throughout FC mode, $Q_{WH,FC}$, is calculated according to Equation 8:

$$Q_{WH,FC} = \sum_{i=1}^{8760} \phi_{CL} + P_{COMP,FC} = \sum_{i=1}^{8760} \phi_{CL} \left(1 + \frac{1}{COP(T_{out})}\right), [kWh] \quad (8)$$

Where $P_{COMP,FC}$ presents water-cooled chiller compressor power and it is calculated using COP value, which is determined by ambient temperature, as shown in Equation 9.

$$P_{COMP,FC} = \frac{\phi_{CL}}{COP(T_{out})}, [kW] \quad (9)$$

The sum of Equations 7 and 8 gives the Total annual waste heat released, Q_{WH} , as shown in Equation 10.

$$Q_{WH} = Q_{WH,FAC} + Q_{WH,FC}, [kWh] \quad (10)$$

3.5. Pinch Method

In this research, two integration technologies were studied:

- Integration of waste heat using a HEX,
- Integration of waste heat using a BHP.

The principle of integration is shown in Figure 6. First, the DHN Return line is coupled with a waste heat integration system where it is first heated in the HEX based on the temperature difference and considering settled conditions. If the heated current reaches the Supply line temperature, then it is injected into the Supply line, if not, the flow is returned to the Return line as preheated which reduces the heat required in the DH central supply unit. If there is a still amount of waste heat that can be integrated into DHN, the BHP is used that ensures that the supply line temperature is achieved. In this paper, the chosen sequence of waste heat integration is as follows: first, waste heat integration using HEX, then using BHP. This makes it possible to integrate high-temperature waste heat, which is suitable for HEX, and then the rest is integrated with BHP, allowing the rise of the temperature level of the remaining waste heat. Integration technology with preheating option is not observed in this paper. Pinch analysis was applied to calculate the amount of waste heat that can be integrated into DHN using HEX and BHP [16].

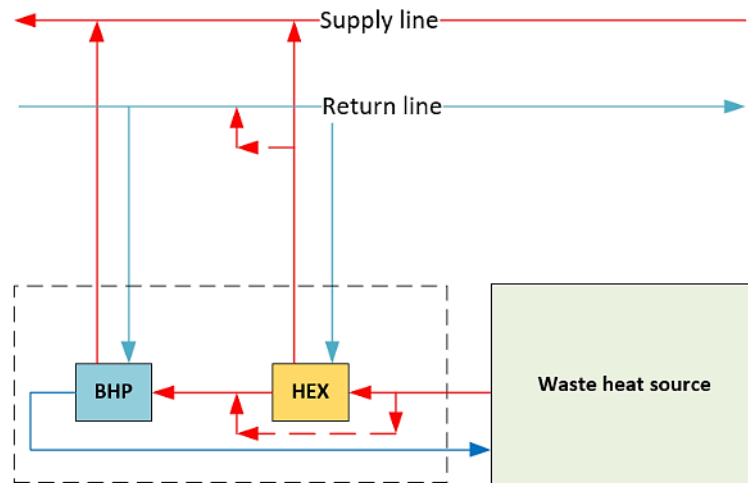


Figure 6 Simplified scheme of the waste heat integration system with HEX and BHP

The temperature regime of the DHN and the amount and temperature of waste heat are the two main input variables in the pinch analysis. Additionally, input on the thermal capacity of the DHN connection, which entails the flow rate through the pipeline and the diameter of the connecting pipe, is needed also. The connecting pipe is a pipe between the HEX or BHP to the DHN. A wider connection pipe diameter allows better thermal flow capacity entering the waste heat integration system, pipe diameter plays a significant role in pinch analysis. By comparing the results of different pipe diameters, pinch analysis can be used to find the ideal diameter of the connection pipe. The amount of waste heat integrated into DHN is the most significant result that can be obtained by combining different input data. A more detailed explanation of the pinch analysis approach could be found in [16].

3.6. Booster heat pump

The BHP rise the temperature of the DH flow using a waste heat source. The heat source is the DC, and the heat sink is the DHN. The BHP is modelled using the Lorentz efficiency model. The method for Lorentz efficiency determination is described in [19].

A general approach is shown in Equation 11 where COP is the computed COP of the BHP and COP_{Lor} is the theoretical Lorenz COP of the BHP. Using Lorenz efficiency, η_{Lor} , the real value is obtained. Equation 12 is used to compute Lorenz COP, COP_{Lor} . where, \bar{T}_H is the mean heat sink temperature and, $\bar{\Delta T}_{lift}$ is the mean heat sink and heat source temperature difference, also known as temperature lift. The mean temperature of the heating source is \bar{T}_C . It should be noted that, as stated in Equation 13, Lorenz efficiency, η_{Lor} , is not constant but instead directly proportional to temperature lift [19], [20].

$$COP = COP_{Lor} \cdot \eta_{Lor}, [-] \quad (11)$$

$$COP_{Lor} = \frac{\bar{T}_H}{\Delta\bar{T}_{lift}} = \frac{\bar{T}_H}{\bar{T}_H - \bar{T}_C} = \frac{\frac{\Delta T_H}{\ln\left(\frac{T_{H,o}}{T_{H,i}}\right)}}{\frac{\Delta T_H}{\ln\left(\frac{T_{H,o}}{T_{H,i}}\right)} - \frac{\Delta T_C}{\ln\left(\frac{T_{C,o}}{T_{C,i}}\right)}}, [-] \quad (12)$$

$$\eta_{Lor} = 0,1312 * \ln(\Delta\bar{T}_{lift}) - 0,0406, [-] \quad (13)$$

3.7. Connection pipe diameter optimization

The optimization of connection capacity is done for pipes with a diameter between DN100 and DN300. The integrated waste heat for each diameter is determined, as shown on the left diagram in Figure 7. The pipe diameter is shown on the X-axis of this diagram, and the amount of total waste heat integrated is shown on the Y-axis. It is evident that as connecting pipe diameter rises, so does the total amount of waste heat integrate. At one point, as the pipe diameter increases, the amount of waste heat integrated becomes saturated. In other words, for a pipe diameter of DN_1 , we can integrate, Q_1 amount of heat, whereas for a pipe diameter of DN_2 , we can integrate, Q_2 amount of waste heat. It is clear that Q_2 is higher than Q_1 , however, this comes at a higher investment cost for the pipe connection. To examine how much is feasible to increase pipe diameter and to still have the increase in integrated heat the ratio of the integrated heat and connection pipe diameter is introduced. In other words, the objective is to find a connection capacity that provides the highest amount of integrated waste heat for the given connection pipe diameter.

To achieve this, the approach shown in Figure 7 is applied. As illustrated on the Y-axis of the right figure, the ratio of heat integrated and diameter, Q/DN , is introduced. This ratio compares integrated waste heat with investment cost (which correlates with pipe diameter) and it represents the efficiency of the investment of the diameter of the connecting pipe [16]. When the ratio is plotted with respect to the pipe diameter, at a certain diameter the maximum value of the ratio appears. The pipe diameter with the maximum Q/DN ratio represents the ideal pipe capacity, Q_{opt}/DN_{opt} . It should be noted that the $Q_1(DN_1) < Q_{opt}(DN_{opt}) < Q_2(DN_2)$. In Figure 7 right diagram, these values are shown.

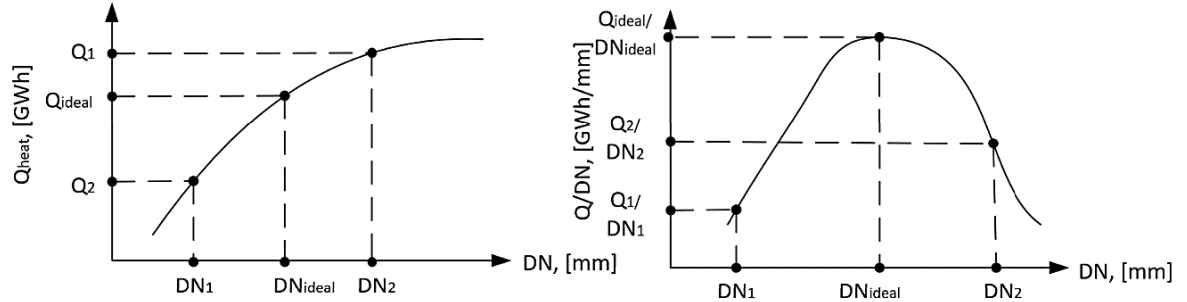


Figure 7 DHN used heat concerning the connection pipe diameter on the left; the ideal DHN connection pipe diameter on the right [16]

3.8. Techno-economic analysis

Considering the Levelized cost approach, the waste heat integration economic viability is evaluated. Equation 14 defines the Levelized Cost of Waste Heat ($LCOWH$).

$$LCOWH = \frac{CAPEX + OPEX}{Q_{WH,integrated}}, \left[\frac{\text{€}}{MWh} \right] \quad (14)$$

Where $Q_{WH,integrated}$ is the Total amount of waste heat integrated into the DHN, $OPEX$ are Operational Expenditures, and $CAPEX$ is Capital Expenditures.

All capital expenditures, i.e., investments. inv , such as the purchase of HEX, BHP, and DHN, are included in $CAPEX$. As shown in Equation 15, capital expenditures have been discounted using the capital recovery factor, CRF , and established discount rate, d .

$$CAPEX = CRF \cdot inv = \frac{d(1+d)^n}{(1+d)^n - 1} \cdot inv, [\text{€}] \quad (15)$$

$OPEX$ is an annual operating expenditure that is not subject to a discount rate. It has both variable and fixed components. The operational and maintenance (O&M) costs of the equipment, as well as the electricity used to power the compressor of the BHP, are variables in the variable component. The fixed portion includes the equipment fixed O&M costs.

In addition to the LCOWH approach, the techno-economic analysis includes the analysis of the potential low-temperature DHN expansion. The potential analysis is based on input data and simple equations that are listed below. The input data are:

- $n_{DH,consumers}$, [-] – total number of consumers in the DH system,
- $Q_{DH,delivered}$, [MWh] – total delivered waste heat via DHN.

From the input data, the waste heat delivered per consumer, $Q_{DH,consumer}$, is calculated:

$$Q_{DH,consumer} = \frac{Q_{DH,delivered}}{n_{DH,consumers}}, [MWh] \quad (16)$$

Since it is known how much waste heat can be integrated into DHN, it is possible to calculate how many consumers can be supplied by integrating the DC as a source of waste heat. This can be calculated as follows:

$$n_{DH,consumers,wh} = \frac{Q_{WH,integrated}}{Q_{DH,consumer}}, [-] \quad (17)$$

This approach introduces some uncertainties. For example, one of the uncertainties is whether consumers have the basic conditions for the application of a low-temperature network, such as the consumer's substation, the condition of the outer envelope, plot ratio, etc.

3.9. Case Study and Input Data

The presented method was tested in the case study of a DC located in the City of Zagreb, Croatia.

To test the method, Approach I was taken. Based on the availability of data and a review of the literature, it is considered that a DC with a capacity of 4MW is sufficient for a city the size of Zagreb. DC with a capacity of 4 MW qualifies as a medium-capacity DC.

The temperature regime of the DHN of the City of Zagreb is currently high temperature, which, according to the literature review, is not suitable for cost-effective integration into the DHN. Therefore, in this research, integration into a low-temperature DHN is considered. Three different low-temperature DH systems were considered:

- LTDH – low-temperature district heating - 60°C/30°C,
- ULTDH – ultra-low temperature district heating - 40°C/20°C,
- NTDH – neutral temperature district heating - 20°C/10°C.

Figure 8 shows the dependence of the DHN temperature on the outdoor temperature.

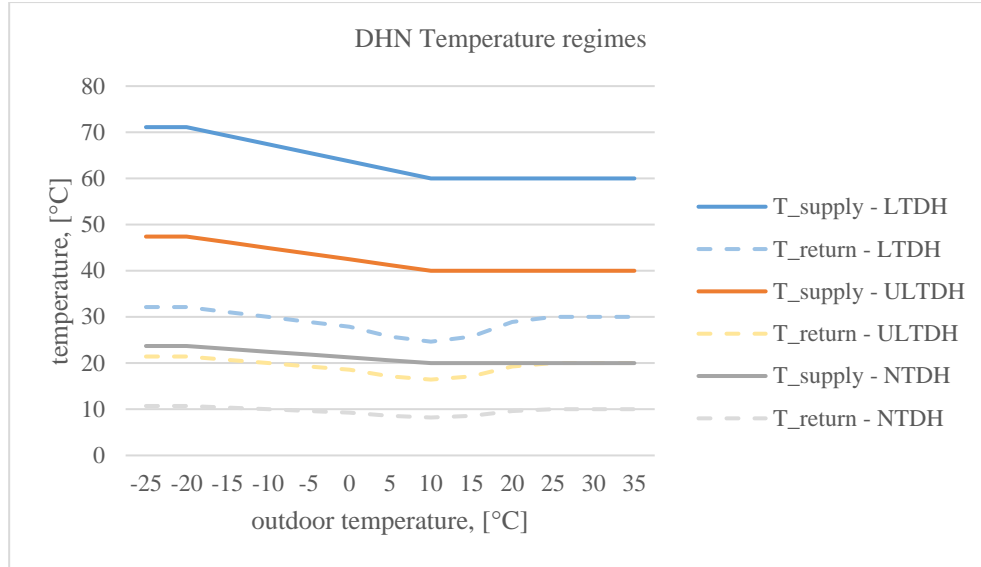


Figure 8 Hourly ambient wet bulb temperature distribution

The average outdoor temperature is observed on an hourly level for the period between 2000 and 2020 [21].

Table 1 shows the input data for the DH connection pipe necessary for pinch analysis.

Table 1 Input data for DH connection pipe

Label	Value	Unit	Name
c_p	4187.00	$[Jkg^{-1}K^{-1}]$	Specific thermal capacity of water
ρ_w	1000.00	$[kg m^{-3}]$	Water density
w_w	1.00	$[m s^{-1}]$	Water flow rate
DN	100 – 300	$[mm]$	Connection pipe diameter

Table 2 shows the fixed input data for the cooling system and the temperature conditions in DC.

Table 2 Input data for the cooling system and DC temperature conditions

Name	Value	Symbol	Unit	Description	Reference
DC hot air aisle	35	$T_{DC,hot}$	$[^{\circ}C]$	Return hot air from the server outlet	[6]
DC cold air aisle	20	$T_{DC,cold}$	$[^{\circ}C]$	Supply cold air on the inlet in the server	[6]
Water inlet temperature	15	$T_{DC,in}$	$[^{\circ}C]$	CRAH inlet water temperature	[17]
Water outlet temperature	22	$T_{DC,out}$	$[^{\circ}C]$	CRAH outlet water temperature	[17]

A COP that depends on outdoor temperatures is used to represent the chiller plant. For the sake of simplicity, it is not considered here how it varies at different loads. The dependence of chiller COP on outdoor temperature is shown in Table 3 [22]. A linear interpolation of the data was used to obtain values between.

Table 3 Water-cooled chiller COP [22], [23]

Outdoor temperature, $[^{\circ}C]$	0	5	10	15	20	25	30	35	40
COP, [-]	5.8	5.5	5.1	4.7	4.34	3.9	3.5	3.1	2.6

Since BHP and HEX are used for the integration of waste heat, it is necessary to determine what their capacities are. The capacity of the selected BHP is 250kW. When selecting the HEX to be installed, attention is paid to the amount of heat that can be integrated using HEX. Thus, the capacity of the HEX is determined by the maximum value of waste that can be integrated into DHN.

Table 4 shows the input data required for techno-economic analysis.

Table 4 Input data for techno-economic analysis

Name	Value	Symbol	Unit	Reference
Discount rate	10	d	[%]	[24]
Life expectancy	20	n	[Year]	-
Part of operative expenditures for HEX into an investment	0.4	γ	[-]	[25]
The specific price of BHP	1.24	c_{BHP}	[MEUR MW ⁻¹]	[26]
Nominal power of BHP	-	$\Phi_{BHP,nom}$	[kW]	-
Fixed operative expenditures for BHP	2.00	$O\&M_{fix}$	[EUR kWh ⁻¹]	[26]
Variable operative expenditures for BHP	2.7	$O\&M_{var}$	[EUR MW ⁻¹ h ⁻¹]	[26]
Electricity for BHP, from the calculation	-	E_{comp}	[MWh]	-
Electricity price for non-households	0.1	c_{elen}	[EUR kWh ⁻¹]	[24]
Specific price for HEX	0.26 * $\Phi_{HEX,nom}^{-0,1234}$	c_{HEX}	[MEUR MW ⁻¹]	[27]
Nominal power for HEX, from load duration of the source	-	$\Phi_{HEX,nom}$	[kW]	-
Total number of consumers in the DH system	113667	$n_{DH,consumers}$	[-]	[28]
Total delivered waste heat via DHN	1539983	$Q_{DH,delivered}$	[MWh]	[28]

4. Results

The results obtained are presented in this chapter. Section 3.1 shows the results of the DC waste heat model, the waste heat distribution curves when the waste heat integration system is installed on the water-cooled chiller condenser side. In addition to the distribution curve, waste heat temperature curves are also shown. Section 3.2 presents the results of the pinch analysis and determined the optimal diameter of the connecting pipe for DHN. Section 3.3 presents the results of the techno-economic analysis for the proposed solution, while Section 3.4 presents the Sensitivity Analysis when changing the price of investment and the price of electricity. In Section 3.5 the Expansion potential of low-temperature DHN is presented.

4.1. Waste heat model

This subsection presents the results of the model described in Section 2. As already mentioned, Approach I of the waste heat model of the DC was chosen. The expected results from the model are the annual distribution of waste heat potential and the temperature of the waste heat source. The model enables knowing the waste heat conditions at any moment of the year on an hourly basis.

Figure 9 shows the results of the DC waste heat model. The orange curve indicates the potential of the waste heat, and the red curve indicates the temperature of the waste heat. The potential of waste heat exists throughout the year since there is a constant need to cool the DC, but this potential may vary throughout the year, which is related to the cooling mode operation. During the winter, when the FAC mode is operational, the waste heat potential is lower, and on average it amounts to 1100 kWh. During FAC mode waste heat temperature is on average 30°C. During the summer it is necessary to use a chiller whose refrigerant allows to achieve higher waste heat potential, as well as temperature. During the period of use of the FC cooling mode, the potential of waste heat can be from 2000 kWh to 7000 kWh, and the temperature can reach values of 55°C.

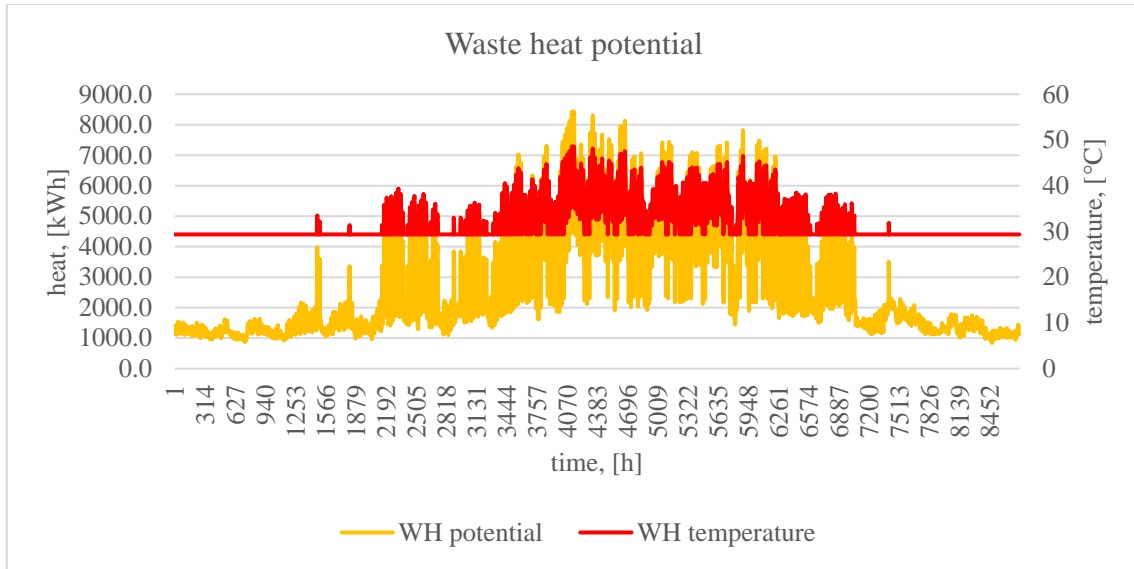


Figure 9 Waste heat potential and temperature

4.2. Pinch analysis

This subsection presents the results of pinch analysis for proposed waste heat recovery technologies. Ways of utilizing waste heat using HEX and BHP are presented with accompanying comments.

Figure 10 shows the results of the pinch analysis for the integration of waste heat into the LTDH network in the winter period (h=8000, month: December) and when the diameter of the connecting pipe is DN300. The dark blue line, marked with *HS*, presents a waste heat source, the red dashed line, marked with *T_{DH,s}*, presents DHN supply flow, the blue dashed line, marked with *T_{DH,r}*, presents DHN return flow, while green line, marked with *BHP*, presents integrated heat into the DHN through BHP. In the period shown in Figure 10, the waste heat source temperature is not high enough to integrate the heat using HEX, and it is necessary to use BHP. A BHP integrates low-temperature waste heat and increases the temperature of return flow to the required supply temperature.

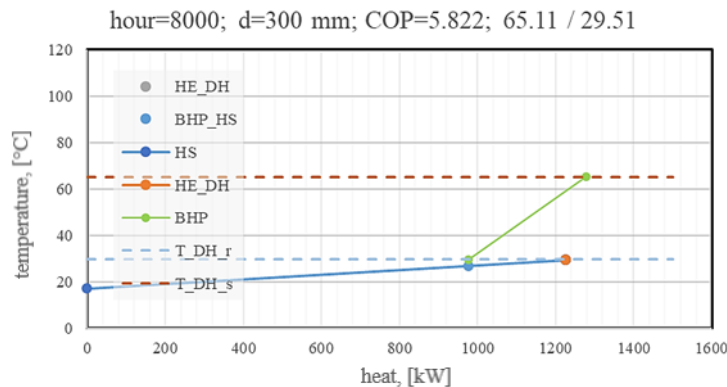


Figure 10 LTDH Pinch analysis – winter period

Figure 11 shows the results of the pinch analysis for the integration of waste heat into the ULTDH network in the winter period on the right (h=50, month: December) and in the summer period on the left (h=4000, month: June). Both, when the diameter of the connecting pipe is DN250. Unlike Figure 10, Figure 11 shows a new orange line, marked with *HE_{DH}*, representing the waste heat integrated through the HEX. Both, on right and left Figures, the source temperature is higher than the temperature in the DHN return flow but lower than the DHN supply flow. The HEX is used for the integration of waste heat to preheat the DHN return flow. The DHN temperature is higher in the right case than in the left case, which is a result of the dependence of the DHN temperature on the outdoor temperature, and thus the temperature is higher in winter and lower in the summer period.

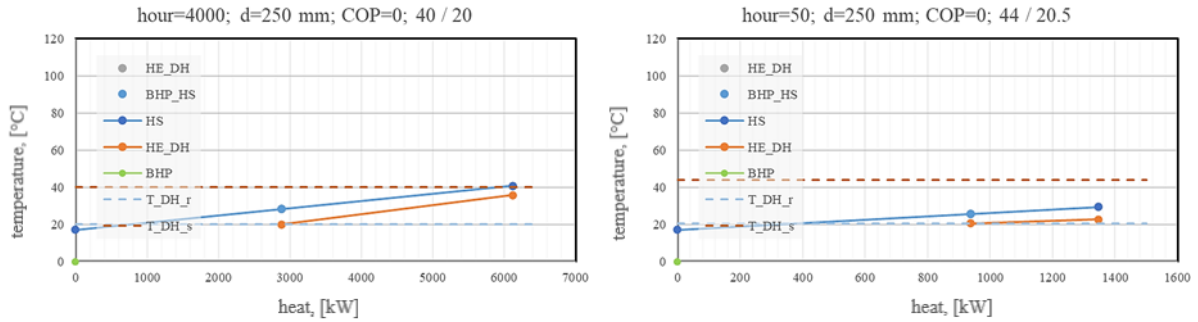


Figure 11 ULTDH Pinch analysis – left - summer period; right - winter period

Figure 12 shows the results of the pinch analysis for the integration of waste heat into the NTDH network in the summer period (h=4400, month: July) on the left and in the winter period (h=8650, month: December) on the right. Both, when the diameter of the connecting pipe is DN225. In both cases, the source temperature is higher than the temperature in the network, so HEX is used for the integration of waste heat. It can be seen from Figure 12 that there is a difference between the left and right cases. In the case on the left, the temperature of the source is higher than both the supply and return flow of the heat network and therefore it is possible to heat the return flow to the required temperature of the supply flow. In the case on the right, it is not possible to heat the return flow to the supply temperature, but only to preheat it.

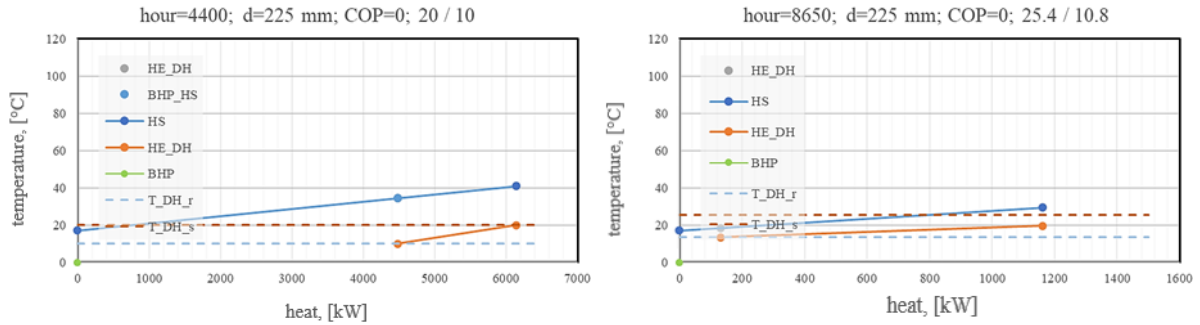


Figure 12 NTDH Pinch analysis – left - summer period; right - winter period

Figure 13 shows the waste heat integrated into the DHN for different connecting pipe diameters and DHN temperature regimes. The left diagram shows the amount of waste heat integrated into DHN when using HEX, while the right diagram shows the waste heat integrated when using BHP. The left diagram shows that the larger connection pipe size enables a higher waste heat amount integration in the DHN when using HEX. Also, the increased integration with the HEX for the specified connection pipe size is possible by decreasing the temperature regime of the DHN. The right diagram shows that the integrated heat is higher in the LTDH network (primary y-axis) than in the ULTDH and NTDH networks (secondary y-axis) when using BHP. However, saturation occurs for the specified boundary conditions, i.e., for pipe sizes wider than DN300. Also, it is noticeable that the BHP integration of the waste heat is lower, when the temperature regime of the DHN is lowered, which is the opposite of the case when using HEX.

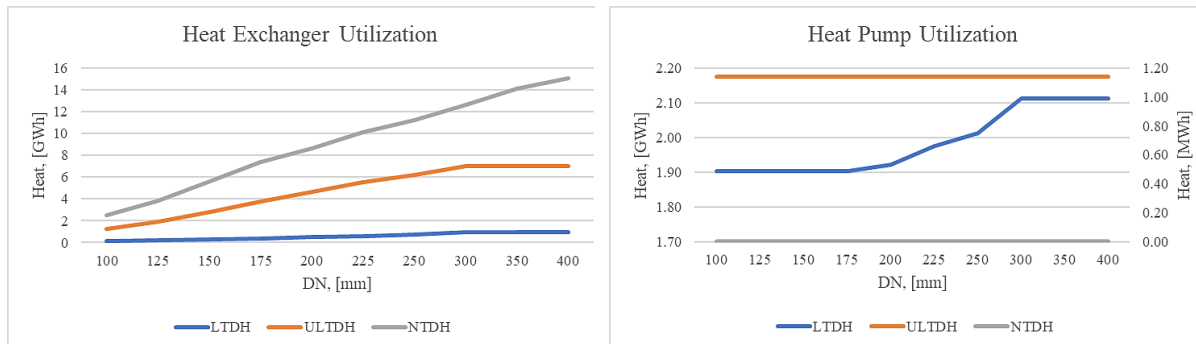


Figure 13 Waste heat integrated into DHN concerning the connection pipe diameter, temperature regime; left – HEX, right – BHP

From the data in Figure 13, we were able to determine the ideal connection pipe diameter. Figure 14 shows a correlation between the connection pipe size (X-axis) and the ratio of integrated heat and diameter (Y-axis). The ratio reaches its maximum value concerning a certain connecting pipe size. This value indicates the ideal diameter used for the techno-economic analysis. The connection pipe size decreases with the reduction of DHN temperature regimes. The optimal value is DN300, 250, and 225 for LTDH, ULTDH, and NTDH. The optimal pipe diameter, together with the maximum ratio values, are indicated in Figure 14.

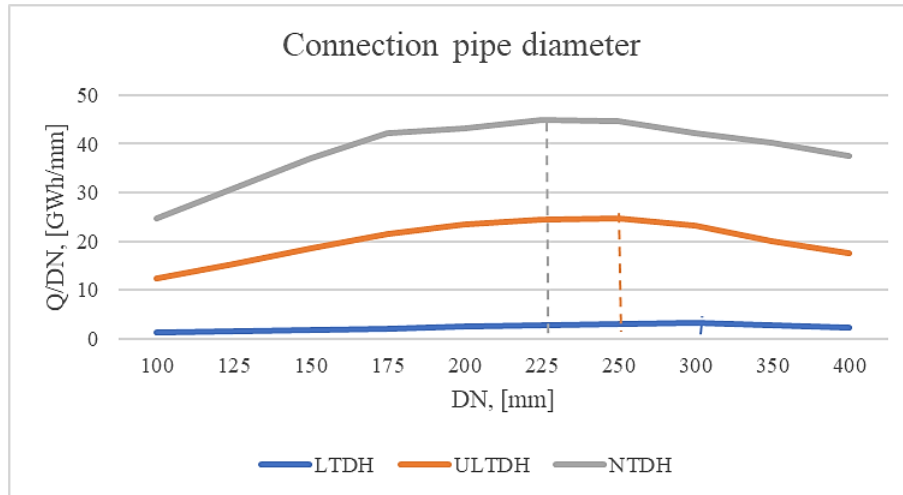


Figure 14 The ratio of integrated heat and diameter regarding different DHN temperature regimes

Table 5 Spectral analysis of the ratio of integrated heat and diameter regarding different DHN temperature regimes

	DN, [mm]	100	125	150	175	200	225	250	300	350	400
$\Phi_{\text{HEX/DN}}$, [GWh/mm]	LTDH	1.23	1.53	1.84	2.15	2.45	2.76	3.07	3.22	2.76	2.41
	ULTDH	12.34	15.43	18.51	21.44	23.40	24.42	24.84	23.32	20.06	17.55
	NTDH	24.76	30.95	37.14	42.33	43.30	44.88	44.79	42.10	40.16	37.57

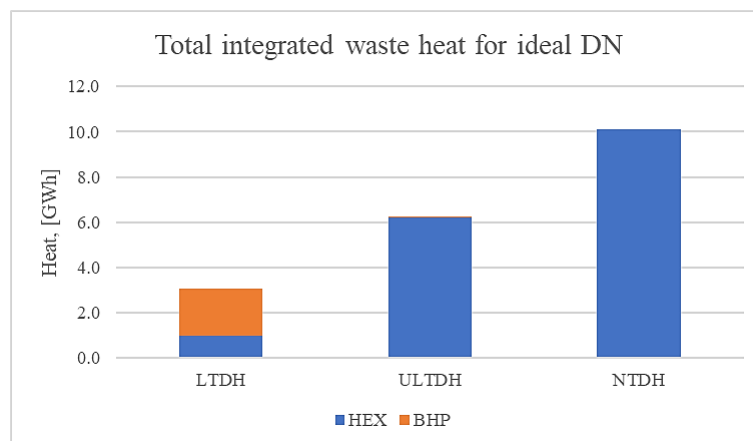


Figure 15 Total integrated waste heat concerning different DHN temperature regimes for ideal DN

The total waste heat injected for different temperature regimes and integration modes is compared in Figure 15. As anticipated, as temperature regimes are lowered, there is a gradual increase in the amount of waste heat that could be utilized directly in heat exchangers. Additionally, as the temperature regime of DHN is lowered, more heat is being used overall in DHN.

4.3. Techno-economic analysis

A techno-economic analysis based on the Levelized Cost of Waste Heat was conducted to compare the outcomes. It is an indication of the price of waste heat integrated into the DHN from the heat sources, i.e., waste heat source. The total cost of the integration system comprises the capital investment expenditures for the

connection pipe and heat integration technology. There are also other operating expenses, such as energy used to power the heat pump compressor, operation, maintenance (fixed and variable), etc.

Figure 16 shows the composition of LCOWH for ideal DN and the length of the connecting pipe 1000m. For this case, LCOWH amounts to 334 €/MWh, 51 €/MWh, and 12.4 €/MWh for LTDH, ULTDH, and NTDH. In the LTDH, the highest cost is the operating cost of BHP and the investment cost of the connecting pipeline. In ULTDH, the highest share of the cost is the investment cost in BHP and the connecting pipeline, while in NTDH the highest amount of the cost is due to the connecting pipeline. Figure 16 shows that the use and integration of waste heat through a BHP significantly increases the LCOWH and makes such a network uncompetitive compared to the DH where the waste heat source is integrated only by using HEX.

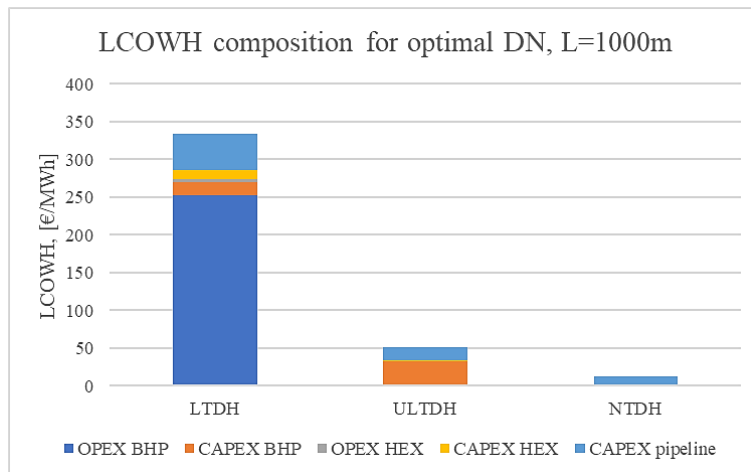


Figure 16 LCOWH composition comparison for ideal DN, L=1000

Figure 17 shows a comparison of the DC LCOWH for different connection pipeline lengths, temperature regimes, and integration technologies. The connection length, which is the distance between the waste heat source and the DHN, raises the cost of heat. Every meter of connection distance necessitates an additional cost, of course. For example, in ULTDH if the waste heat source is near the DHN it can be assumed that the connection length is 0 m and then the LCOWH amounts to 34.4 €/MWh, while if the waste heat source is distant from DHN, i.e., connection length is 1000 m LCOWH can amount for 51 €/MWh, which is higher for 32% then in the case when the connection length is 0 m. In **Pogreška! Izvor reference nije pronađen.** the spectral analysis of above mentioned is shown. Also, based on Figure 16 and Figure 17 the reduction of DHN temperature regimes lowers the LCOWH. Reduction of the temperature regime allows higher waste heat integration which then lowers the LCOWH.

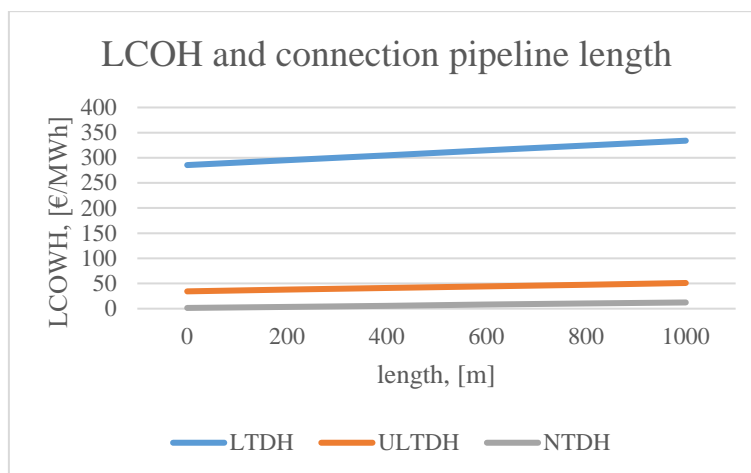


Figure 17 LCOWH considering different connection distances L

Table 6 Spectral analysis of the LCOWH considering different connection distances, L

	Lenght, [m]	0	200	400	600	800	1000
LCOH, [€/MWh]	LTDH	285.47	295.17	304.86	314.56	324.26	333.95
	ULTDH	34.43	37.76	41.09	44.42	47.75	51.08
	NTDH	1.49	3.67	5.85	8.03	10.21	12.39

Changing the length of the connecting pipeline affects the LCOWH differently in a network with high or low-temperature regimes. Thus, the change in the connecting pipeline length affects the LCOWH less in a network with high-temperature regimes than in a network with low-temperature regimes. For example, in the LTDH network, LCOWH for 0 m is 285.47 €/MWh, and for 1000 m it is 333.95 €/MWh, which is a change of 15%. While, for the NTDH network, the length of the connecting pipeline 0 m LCOWH is 1.49 €/MWh, and for 1000 m 12.39 €/MWh, which is a change of almost 88%. This is visible in **Pogreška! Izvor reference nije pronađen.** which shows a spectral analysis of the connection length change.

4.4. Sensitivity analysis

The sensitivity analysis of the Levelized cost of Waste Heat was carried out for two groups of variables:

- Cost of investment and electricity price,
- The discount rate and Life expectancy of equipment.

A sensitivity analysis was performed for all three observed low-temperature DH regimes.

Figure 18 and Figure 19 show the sensitivity analysis of the LCOWH to changes in the investment cost and the price of electricity. Due to the higher LCOWH for LTDH, the display of the sensitivity analysis is divided into Figures correlating with LTDH and Figures correlating with ULTDH and NTDH network.

Figure 18 shows the sensitivity analysis of the waste heat integration in the LTDH network. The figure shows that by changing the investment cost by +/- 20%, the LCOWH changes by +/- 5%, i.e., when the investment cost is reduced the LCOWH amounts to 317.72 €/MWh, while for an increase the LCOWH amounts to 350.18 €/MWh. Electricity price change for +/- 20% results in LCOWH change for +/- 1%. In the case of a lower price the LCOWH amounts to 330.81 €/MWh, and in the case of a price increase the LCOWH amounts to 337.1 €/MWh. According to Figure 18, the LTDH network is more sensitive to the investment cost change than to the electricity price change.

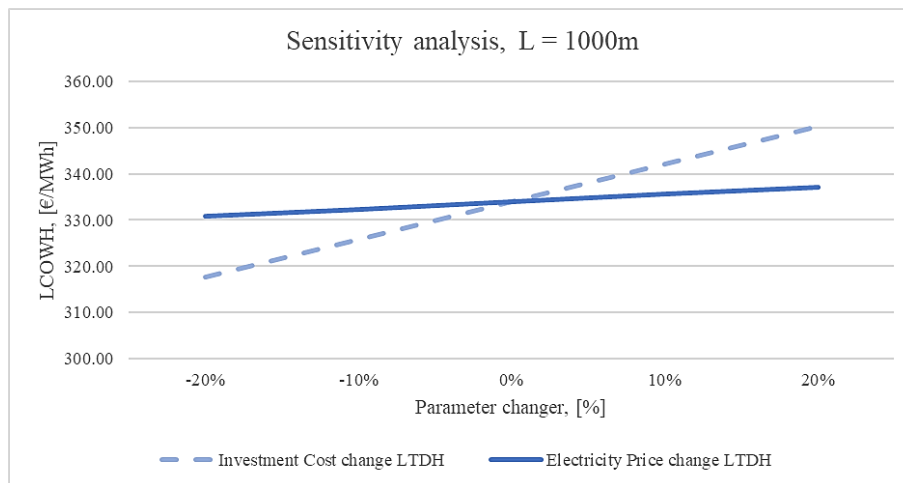


Figure 18 LTDH - Sensitivity analysis for DN 300, L = 1000 m

Figure 19 shows the sensitivity analysis of the waste heat integration in the ULTDH and NTDH networks. By changing the investment cost by +/- 20%, the LCOWH in the ULTDH network amounts to 20% less and it amounts to 40.88 €/MWh if the investment cost is reduced. If the cost is increased, the LCOWH rises by 17% and amounts to 61.29 €/MWh. When the price of electricity changes, the sensitivity is very slight, i.e., negligible. The reason behind this is because the integration of waste heat in this type of network is usually with HEX, which

requires less electricity for operation than is the case with BHP. In the NTDH system, a change in the investment cost, i.e., by reducing the cost, the LCOWH is reduced by 20% and it amounts to 9.91 €/MWh, while if the price increase, the LCOWH is 17% higher, i.e., it amounts to 14.87 €/MWh. The NTDH network isn't sensitive to the electricity price change and there is no impact on the LCOWH because the integration of waste heat takes place via HEX.

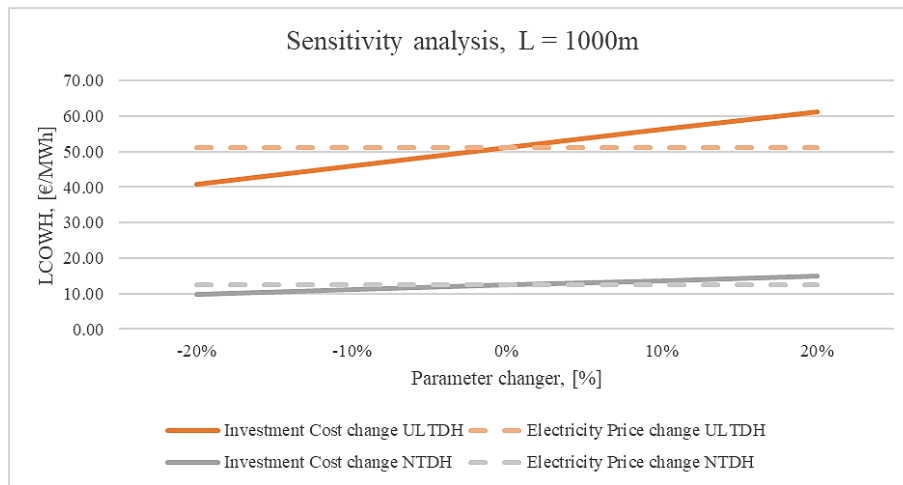


Figure 19 ULTDH & NTDH - Sensitivity analysis for ideal DN, L = 1000 m

Figure 20 and Figure 21 show the sensitivity analysis of the waste heat integration regarding the change in the discount rate and the expected lifetime of the equipment. Figure 20 shows the sensitivity analysis of the waste heat integration in the LTDH network. By changing the discount rate by +/- 50%, the LCOWH changes by +/- 8%. When the discount rate decreases the LCOWH amounts to 309.48 €/MWh, and when the discount rate rises, the LCOWH amounts to 361.77 €/MWh. A change in the expected life of the equipment by +/- 50% has a polynomial character of the curve, and when the expected life decreases, the LCOWH rises by 9% to 363.73 €/MWh, while if the expected life increases, the LCOWH decreases by 2% and amounts 326.47 €/MWh. From Figure 20 it is obvious that the LCOWH is more sensitive when the expected life of the equipment is shorter the LCOWH increase, while in the case of extending the expected life, the LCOWH decrease but to a lesser extent.

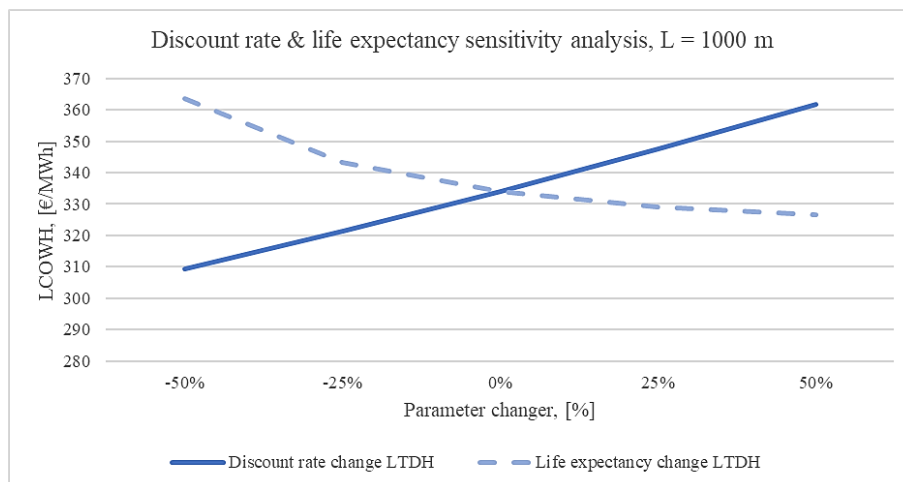


Figure 20 LTDH – Discount rate and Life expectancy analysis for DN 300, L = 1000 m

Figure 21 Figure 20 shows the sensitivity analysis of the waste heat integration in the ULTDH and NTDH networks. First, an explanation is given for the ULTDH network, and then for the NTDH network. Figure 21 shows that a change in the discount rate has a high impact on the ULTDH network. If the discount rate is lower, the LCOWH decreases by 31% and amounts to 35.12 €/MWh. If the discount rate is higher, the LCOWH increases by 26% and amounts to 69.23 €/MWh. The change in the expected equipment life has a significant impact on the LCOWH. For a shorter equipment life, the LCOWH increases by 38% and reaches 70.51 €/MWh, while if the equipment life is longer, it increases by 11% and reaches 46.2 €/MWh. The LCOWH in the NTDH network shows

a similar character. In the case of a lower discount rate, the LCOWH rises by 31% and amounts to 8.58 €/MWh, while if the discount rate is higher, the LCOWH rises by 26% and amounts to 69.23 €/MWh. By shortening the expected life of the equipment LCOWH increases by 37% and reaches 17.02 €/MWh, and by extending it the LCOWH is 10% higher and reaches 11.22 €/MWh. Therefore, as in the case of the LTDH network, the LCOWH in the ULTDH and NTDH networks is more sensitive when the expected life of the equipment is shorter. By shortening the expected life of the equipment, the LCOWH increases, while in the case of extending it, the LCOWH decreases to a lesser extent. Considering the above, the sensitivity analysis in ULTDH and NTDH have a similar character when changing the discount rate and the expected life of the equipment.

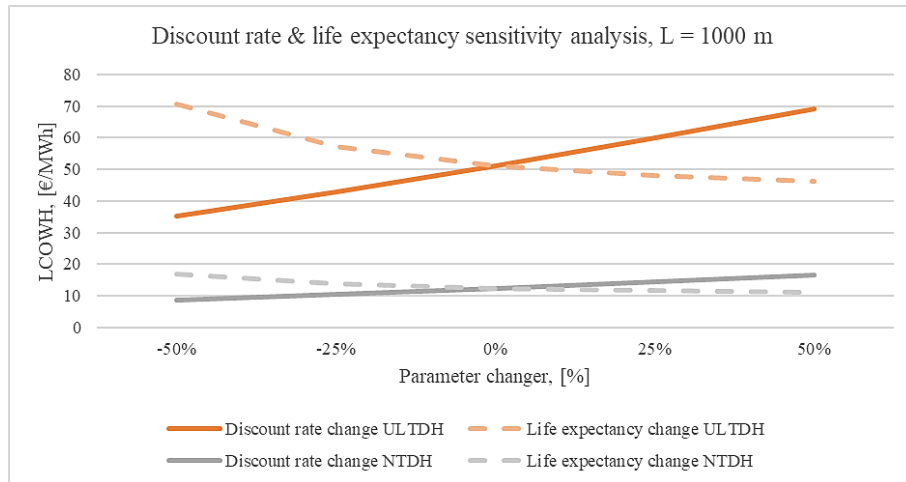


Figure 21 ULTDH & NTDH – Discount rate and Life expectancy analysis for ideal DN, $L = 1000\text{ m}$

To summarize, the sensitivity analysis showed that lowering the temperature regime of the DHN leads to an increase in the sensitivity of the waste heat integration in the context of the investment cost, the discount rate, and the expected life of the equipment change. The only exception is the price of electricity change regarding the waste heat integration into the LTDH network. In this scenario, sensitivity occurs, while the ULTDH and NTDH networks don't show sensitivity, due to the consumption of electricity for the BHP compressor operation.

4.5. The expansion potential of low-temperature district heating systems

Table 7 shows the analysis of the potential for expansion, i.e., for covering the heat load of consumers by integrating waste heat from the DC. Reducing the temperature regime allows the integration of a larger amount of waste heat, so it is expected that the number of consumers that can cover the heat load rise. According to Table 7, NTDH shows the highest potential, while LTDH has the lowest expansion potential.

Table 7 DH system expansion potential

	LTDH	ULTDH	NTDH
$n_{DH,consumers}$, [-]	113667		
$Q_{DH,delivered}$, [MWh]	1539983		
$\frac{Q_{DH,delivered}}{n_{DH,consumer}}$, [$\frac{MWh}{consumer}$]	13.55		
$Q_{DH,recovered}$, [MWh]	3077.44	6209.98	10097.4
$n_{DH,consumer,wh}$, [-]	227.15	458.36	745.3

5. Conclusion

The integration of waste heat from DC into DH systems today is becoming important due to the opportunity to increase energy efficiency, reduce dependence on fossil fuels, i.e., decarbonize energy systems, and rationalize the use of resources. DC are energy systems that have a high energy density and offer many opportunities in the electricity sector, but also in the heating sector as they can provide significant amounts of waste heat at medium-high temperatures. The trend in DH is lowering the temperature regime, which gives a new opportunity to urban heat sources, but especially to DC.

In this research the techno-economic optimization of the DC waste integration into low-temperature DHN. The thermodynamic model of the DC which provides data on waste heat potential and temperature level on an hourly level is developed. An hourly merit order model based on pinch analysis is developed and adapted to be suitable for thermodynamic model integration. The developed model considers both waste heat source and DHN temperature regimes. Two integration technologies are examined: HEX and BHP. By carrying out a series of simulations with different connection pipe sizes, an ideal connection capacity for each temperature regime is obtained. To test the method, a fictitious DC located in the City of Zagreb is considered. The obtained results show that the ideal diameter of the connecting pipe is DN300, DN250, and DN225 for LTDH, ULTDH, and NTDH networks. Techno-economic analysis has shown that recovery of waste heat is economically viable if the temperature regime of the DHN is lower. The research showed that the integration of the waste heat into the LTDH network is more expensive than the integration into the ULTDH and NTDH networks which is caused by the high operational cost of the booster heat pump. The research showed that reducing the temperature regime of the DH makes the integration of the DC waste heat less expensive due to the cheaper integration technology with lower capital and operational cost. Furthermore, a sensitivity analysis is carried out that showed that the DC waste heat integration is sensitive to investment cost, the discount rate, and the expected life of the equipment change, while the electricity price change has a significant role only in the waste heat integration into the LTDH network. Finally, the techno-economic analysis showed that the NTDH network has the highest potential to cover the heat load of the consumers, i.e., to integrate new consumers into the DHN due to the highest amount of the waste heat integrated.

In the future, it is proposed to expand the research to consider the environmental impact of the integration of waste heat from DC in terms of CO₂ emission reduction, energy consumption, and application of DC energy metrics such as Power Usage Efficiency (PUE), Energy Recovery Efficiency (ERE), Energy Recovery Factor (ERF), etc. In future work, it is aimed to expand the pinch model by adding more substation variations. Also, it is necessary to consider a more detailed approach to examine the potential for network integration or expansion.

Acknowledgment: We would like to express our gratitude to the consortium of the REWARDHeat (Renewable and Waste Heat Recovery for Competitive District Heating and Cooling Networks) Horizon2020 project, Grant Agreement no. 857811. Also, we would like to express our gratitude to the Croatian Science Foundation.

6. Literature

- [1] G. Thomaßen, K. Kavvadias, and J. P. Jiménez Navarro, “The decarbonisation of the EU heating sector through electrification: A parametric analysis,” *Energy Policy*, vol. 148, p. 111929, Jan. 2021, doi: 10.1016/J.ENPOL.2020.111929.
- [2] N. Bertelsen and B. V. Mathiesen, “EU-28 residential heat supply and consumption: Historical development and status,” *Energies (Basel)*, vol. 13, no. 8, Apr. 2020, doi: 10.3390/en13081894.
- [3] E. Wheatcroft, H. Wynn, K. Lygnerud, G. Bonvicini, and D. Leonte, “The role of low temperature waste heat recovery in achieving 2050 goals: A policy positioning paper,” *Energies (Basel)*, vol. 13, no. 8, Apr. 2020, doi: 10.3390/en13082107.
- [4] H. Fuchs *et al.*, “Comparing datasets of volume servers to illuminate their energy use in data centers,” *Energy Effic*, vol. 13, no. 3, pp. 379–392, Mar. 2020, doi: 10.1007/s12053-019-09809-8.
- [5] L. Fu, Y. Li, Y. Wu, X. Wang, and Y. Jiang, “Low carbon district heating in China in 2025- a district heating mode with low grade waste heat as heat source,” *Energy*, vol. 230, p. 120765, Sep. 2021, doi: 10.1016/J.ENERGY.2021.120765.
- [6] K. Ebrahimi, G. F. Jones, and A. S. Fleischer, “A review of data center cooling technology, operating conditions and the corresponding low-grade waste heat recovery opportunities,” *Renewable and Sustainable Energy Reviews*, vol. 31. Elsevier Ltd, pp. 622–638, 2014. doi: 10.1016/j.rser.2013.12.007.
- [7] N. Rasmussen, “Guidelines for Specification of Data Center Power Density White paper | Schneider Electric,” *Schneider Electric Science Center*, 2011. https://www.se.com/id/en/download/document/SPD_NRAN-69ANM9_EN/ (accessed Dec. 14, 2021).

- [8] P. Huang *et al.*, “A review of data centers as prosumers in district energy systems: Renewable energy integration and waste heat reuse for district heating,” *Applied Energy*, vol. 258. Elsevier Ltd, Jan. 15, 2020. doi: 10.1016/j.apenergy.2019.114109.
- [9] E. Oró, P. Taddeo, and J. Salom, “Waste heat recovery from urban air cooled data centres to increase energy efficiency of district heating networks,” *Sustain Cities Soc*, vol. 45, pp. 522–542, Feb. 2019, doi: 10.1016/J.SCS.2018.12.012.
- [10] G. Lennermo, P. Lauenburg, and S. Werner, “Control of decentralised solar district heating,” *Solar Energy*, vol. 179, pp. 307–315, Feb. 2019, doi: 10.1016/J.SOLENER.2018.12.080.
- [11] J. Li, Z. Yang, H. Li, S. Hu, Y. Duan, and J. Yan, “Optimal schemes and benefits of recovering waste heat from data center for district heating by CO₂ transcritical heat pumps,” *Energy Convers Manag*, vol. 245, Oct. 2021, doi: 10.1016/j.enconman.2021.114591.
- [12] G. F. Davies, G. G. Maidment, and R. M. Tozer, “Using data centres for combined heating and cooling: An investigation for London,” *Appl Therm Eng*, vol. 94, pp. 296–304, Feb. 2016, doi: 10.1016/J.APPLTHERMALENG.2015.09.111.
- [13] M. Wahlroos, M. Pärssinen, J. Manner, and S. Syri, “Utilizing data center waste heat in district heating – Impacts on energy efficiency and prospects for low-temperature district heating networks,” *Energy*, vol. 140, pp. 1228–1238, 2017, doi: 10.1016/j.energy.2017.08.078.
- [14] M. Wahlroos, M. Pärssinen, S. Rinne, S. Syri, and J. Manner, “Future views on waste heat utilization – Case of data centers in Northern Europe,” *Renewable and Sustainable Energy Reviews*, vol. 82, pp. 1749–1764, Feb. 2018, doi: 10.1016/j.rser.2017.10.058.
- [15] M. Deymi-Dashtebayaz and S. Valipour-Namanlo, “Thermoeconomic and environmental feasibility of waste heat recovery of a data center using air source heat pump,” *J Clean Prod*, vol. 219, pp. 117–126, May 2019, doi: 10.1016/J.JCLEPRO.2019.02.061.
- [16] H. Dorotić, K. Čuljak, J. Miškić, T. Pukšec, and N. Duić, “Technical and Economic Assessment of Supermarket and Power Substation Waste Heat Integration into Existing District Heating Systems,” *Energies 2022, Vol. 15, Page 1666*, vol. 15, no. 5, p. 1666, Feb. 2022, doi: 10.3390/EN15051666.
- [17] J. Li, J. Jurasz, H. Li, W. Q. Tao, Y. Duan, and J. Yan, “A new indicator for a fair comparison on the energy performance of data centers,” *Appl Energy*, vol. 276, p. 115497, Oct. 2020, doi: 10.1016/J.APENERGY.2020.115497.
- [18] G. Ghatikar *et al.*, “Demand Response and Open Automated Demand Response Opportunities for Data Centers,” Berkeley, CA (United States), Dec. 2009. doi: 10.2172/981725.
- [19] J. K. Jensen, T. Ommen, L. Reinholdt, W. B. Markussen, and B. Elmegaard, “Heat pump COP, part 2: Generalized COP estimation of heat pump processes,” *Refrigeration Science and Technology*, vol. 2018-June, pp. 1255–1264, 2018, doi: 10.18462/iir.gl.2018.1386.
- [20] Danish Energy Agency, “Technology Data-Energy Plants for Electricity and District heating generation,” Copenhagen, Aug. 2016. [Online]. Available: <http://www.ens.dk/teknologikatalog>
- [21] European Commission and Joint Research Centre, “JRC Photovoltaic Geographical Information System (PVGIS),” 2017. https://re.jrc.ec.europa.eu/pvg_tools/en/ (accessed May 05, 2022).
- [22] TRANE, “Air-Cooled Series R™ Helical-Rotary Liquid Chiller - Model RTAC 120 to 400 (400 to 1500 kW-50 Hz) Built for the Industrial and Commercial Markets,” Brussels, Oct. 2010.
- [23] J. Salom, L. Sisó, and M. Sansigre, “Cost-Effective Renewable Cooling on Green Data Centres,” Barcelona, Dec. 2014.
- [24] “Home - Eurostat.” <https://ec.europa.eu/eurostat> (accessed May 05, 2022).

- [25] S. A. Aromada, N. H. Eldrup, F. Normann, and L. E. Øi, “Techno-Economic Assessment of Different Heat Exchangers for CO₂ Capture,” *Energies* 2020, Vol. 13, Page 6315, vol. 13, no. 23, p. 6315, Nov. 2020, doi: 10.3390/EN13236315.
- [26] “Technology Data for Generation of Electricity and District Heating | Energistyrelsen.” <https://ens.dk/en/our-services/projections-and-models/technology-data/technology-data-generation-electricity-and> (accessed May 05, 2022).
- [27] I. Best, J. Orozaliyev, and K. Vajen, “Economic comparison of low-temperature and ultra-low-temperature district heating for new building developments with low heat demand densities in Germany,” *International Journal of Sustainable Energy Planning and Management*, vol. 16, pp. 45–60, May 2018, doi: 10.5278/IJSEPM.2018.16.4.
- [28] “ENERGIJA U HRVATSKOJ 2020. I ENERGY IN CROATIA 2020 PREDGOVOR I FOREWORD ENERGY IN CROATIA 2020.”